Electronic structures of N- and C-doped NiO from first-principles calculations

The SEC Strategic Research Cluster and the Centre for Synthesis and Chemical Biology, Conway Institute of Biomolecular and Biomedical Research, School of Chemical and Bioprocess Engineering, University College Dublin, Belfield, Dublin 4, Ireland

Run Long, Niall J. English[a)] and Damian A. Mooney

Abstract: The large intrinsic band gap of NiO has hindered severely its potential application under visible-light irradiation. In this study, we have performed first-principles calculations on the electronic properties of N- and C-doped NiO to ascertain if its band gap may be narrowed theoretically. It was found that impurity bands driven by N 2p or C 2p states appear in the band gap of NiO and that some of these locate at the conduction band minimum, which leads to a significant band gap narrowing. Our results show that N-doped NiO may serve as a potential photocatalyst relative to C-doped NiO, due to the presence of some recombination centres in C-doped NiO.

Keywords: doped, electronic structure, NiO

[a)] Corresponding author. Electronic Mail: niall.english@ucd.ie

1. Introduction

Metal oxides have a wide application in the area of gas sensors, catalysis, photochemistry, and electrochemistry [1, 2]. Among them, titania (TiO_2)-based materials have received the most attention as promising photocatalytic materials for the decomposition of organic pollutants present in water or air, due chiefly to their low cost, nontoxicity, long-term stability and high oxidative power. However, their universal use is restricted to ultraviolent light ($\lambda < 385$ nm) due to the wide band gap of titania (~3.2 eV for anatase and 3.05 eV for rutile). In general, doping is one of the most effective approaches to extend the absorption edge to visible-light range. For example, N-doped TiO_2 is considered to be a promising photocatalyst, and it has been investigated widely, both by experimental and theoretical methods [3, 4]. In addition to N-doped TiO_2, C-doped TiO_2 also shows good photocatalytic efficiency under visible-light [5].

Besides TiO_2, NiO is also of interest as a catalyst for electrochemical applications like electrolysers, fuel cells, and batteries [6, 7]. NiO-loaded semiconductors have been used extensively as photocatalysts for water splitting due to the metal support interface being an important factor affecting the efficiency of the process. The pioneering work done by Zou et al. [8] introduced water splitting for stoichiometric H_2 and O_2 evolution over $NiO_x/In_{0.9}Ni_{0.1}TaO_4$ photocatalysts under visible light irradiation. Following this work, Hu et al. [9] reported that $NiO/SrBi_2O_4$ could effectively decompose pathogenic bacteria under visible light irradiation. Liu et al. [10] controlled the metal support interfaces of NiO-loaded photocatalysts such as

NiO/Ta_2O_5 and NiO/ZrO_2 prepared with plasma treatment, to exhibit high activity for photocatalytic hydrogen generation from pure water and methanol solution, respectively. On the other hand, the investigation of $NiO/NiAl_2O_4$ as oxygen carriers for chemical-looping combustion to fabricate high effective gaseous fuels has been investigated by several groups [11, 12]. However, the band gap of pure NiO is 3.8 eV experimentally, which is still very large and only active in the UV region [13]. So, to shift the photon absorption edge to the visible light region and thus improve its efficiency, it is reasonable to speculate that doping with non-metal elements, such as N or C, may narrow its band gap and achieve this aim. In the absence of experimental data, theoretical investigation could give meaningful qualitative results and help to guide future experimental work.

In the present study, our aim is to investigate how to modify the electronic structure of NiO via substitutional N and C doping based on first-principles calculations. We find that N 2p states are located just above the valence band maximum (VBM) and lower the conduction band minimum (CBM) of NiO, therefore contributing to a shift of photoreactivity to a lower energy. For C-doped NiO, the C 2p states also appear in the band gap, and thus C-doped NiO may be unsuitable for photocatalyltic materials due to the possibility of C 2p states acting as recombination centres.

2. **Methodology**

All of the spin-polarized DFT calculations were performed using the projector augmented wave (PAW) pseudopotentials as implemented in the Vienna ab initio

Simulation Package (VASP) code [14, 15]. The Perdew and Wang parameterization [16] of the generalized gradient approximation (GGA) [17] was adopted for the exchange-correlation potential. The electron wave function was expanded in plane waves up to a cutoff energy of 400 eV and a Monkhorst–Pack *k*-point mesh [18] of 4 × 4 × 4 was used for geometry optimization and electronic property calculations. Both atomic positions and cell parameters were optimized until the residual forces were below 0.01 eV/Å. Because of strong on-site Coulombic repulsion between Ni 3d electrons, standard density functional theory (DFT) cannot describe properly the physical properties of NiO; the most obvious shortcoming is underestimation of the band gap. However, DFT+U [19, 20] and the hybrid functional B3LYP [21] can lead to a significantly improved and consistent description of the electronic structure of NiO [19, 20]. For the sake of saving computational cost and still keeping the correct description of NiO electronic properties, here, we used the DFT+U method, with U = 5.3 eV. Here, U= U' – J, and U'= 6.3 eV is the Hubbard parameter with J = 1eV as the exchange parameter; U is the effective on-site Coulombic repulsion parameter. This was applied to Ni 3d electrons, based on previous recommendations [20].

The doping systems were constructed from the relaxed (2 × 2 × 2) 64-atom NiO supercell. A single O atom was replaced by a single X (C, N), corresponding to 1.56 atom % N or C concentration. The supercell system is shown in Figure 1.

3. Results and discussion

We first calculated the properties of pure NiO to compare with experimental values

in Table 1. The calculated band gap is 2.6 eV and the lattice value is 4.16 Å, which agrees reasonably with the experimental band gap of 3.8 eV [13] and the lattice constant of 4.17 Å [22]. The calculated local magnetic moment on the Ni ion is 1.68 μ_B, which is consistent with 1.64 μ_B in experiment [23]. The band gap is also consistent with the previous estimate of 3.1 eV from GGA + U but significantly better relative to the 0.5 eV value from the GGA method [20]. Furthermore, d states of Ni locate above O 2p states, which agree with the photoemission data [22, 24]. This suggests that our theoretical method is reasonable.

Secondly, we investigated the energetic difficulty of incorporation of the dopants N and C into the NiO lattice. The dopants' formation energies were calculated according to formula (1) below

$$E_{form} = E(X@O) - E(NiO) - \mu_X + \mu_O \quad (1)$$

where $E(X@O)$ is the total system energy containing substitutional impurities (X= C, N) and $E(NiO)$ is the total energy of the pure 64-atom NiO supercell. μ_O (μ_{Ni}) is the chemical potential for O (Ni). It should be noted that the formation energy depends on the growth conditions, which can be varied from O- to Ni-rich, and satisfy the relationship $\mu_{Ni} + \mu_O = \mu_{NiO}$. Under O-rich conditions, the chemical potential μ_O is determined by the energy of an O_2 molecule and μ_{Ni} is calculated by the above formula. Under Ni-rich conditions, μ_{Ni} amounts to the energy of one Ni atom in bulk Ni ($\mu_{Ni} = \mu_{Ni}^{metal}$) and μ_O is determined based on the previous formula. For C and N dopants, the chemical potentials μ_C and μ_N were determined by $\mu_C = \mu(CO_2) - 2\mu_O$ and $\mu_N = \mu(NO_2) - 2\mu_O$, respectively. This method was used to

discuss the formation energies in N and/or W doped TiO_2 [25]. The calculated formation energies under Ni- and O-rich growth conditions are summarized in Table 2. Their order suggests that: 1) substitutional replacement of O by N is energetically preferable to substitution of O by C under both Ni- and O-rich growth conditions; 2) substitution of N or C in place of O is energetically favorable in Ni-rich conditions vis-à-vis O-rich conditions. There are two possible reasons responsible for these formation energy results. The first is that the ionic radii are in the order C (2.60 Å) > N (1.71 Å) > O (1.40 Å) [26], suggesting that replacement of O by N is easier than by C. The second possibility is the elements' electronegativities are in the order C (2.55) > N (3.04) > O (3.44) [26], implying that the formation of N-Ni bonds is achieved more easily than the formation of C-Ni bonds. The optimized average C-Ni and N-Ni bond lengths are 2.026 and 2.045 Å, respectively; the former occurs due to a large local structure distortion relative to the latter case compared with the optimized O-Ni bond length. This indicates also that incorporation of a relatively larger C into the NiO lattice requires more energy. In addition, the calculated Bader charges [27] on N and C are -1.48|e| and -1.01|e|, indicating that the impurities N and C exist as anions in N- and C-doped NiO.

Following these energetic and structural considerations, we investigated how to modify the band gap of TiO_2 via N or C doping. To accomplish this, knowledge of the characteristics of the band structure in pure NiO is needed. The density of states (DOS) and projected DOS (PDOS) of pure NiO from GGA + U calculations are plotted in Figures 2 (a) and (b), respectively. They show that the top of the valence band is

composed mainly of O 2p states and that the bottom of the conduction band is dominated by Ni 3d orbitals, which is similar to titania, in which the top of the valence band consists essentially of O 2p states and Ti 3d occupies mainly the bottom of the conduction band [3]. It may be expected that C and N would modify the valence band edge (p-type doping) or introduce impurity states into the band gap because of different p orbitals arising between C, N and O atoms.

The calculated DOS and PDOS of N- and C-doped NiO are shown in Figure 3. For N-doped NiO (cf. Figure 3a and 3a'), we find that the bands originating from N 2p states locate just above the VBM of NiO while less N 2p states locate at the CBM simultaneously. On the other hand, the Fermi level E_F located above the N 2p states means that these impurity bands are fully occupied and cannot act as recombination stites. This would serve to reduce the photon transition energy significantly for electron transfer from these states to the CBM. This process induces a narrowing of the band gap, leading to a value of 1.3 eV which is significantly smaller than that of pure NiO (2.6 eV). For C-doped NiO (cf. Figures 3b and 3b'), there are some impurity bands introduced above the VBM while some lie in the band gap; further, some of these locate below the CBM. All of these lead to a significant reduction in the band gap to a value of around 1.3 eV. However, it should be noted that the Fermi level E_F is pinned to the gap states, which means that these states below the E_F are fully occupied and are empty above the E_F. Further, the empty states could serve to act as recombination centres of charge carriers, thereby reducing the photocatalytic efficiency under visible-light irradiation. Although C-doped NiO has a relatively

smaller band gap than N-doped NiO, it would be expected the C-doped NiO would not be suitable for use as a viable visible-light photocatalyst due to the presence of recombination centres. The electronic structure of N-doped NiO is very similar to N-doped TiO_2 [25], which implies that N-doped NiO also has the potential to be an effective photocatalyst under visible-light irradiation. Further, C 2p acceptor states [cf. Figures 3 (b) and (b')] lie deeper inside the gap than those of N 2p acceptor states [cf. Figures 3(a) and (a')] because the C 2p orbital energy is higher than that of N 2p. In addition, there are one and two less valence electrons for N and C than O, respectively, so that replacement O by N and C implies electron-doping resulting in an upshift of the Fermi level of doped systems with respect to pure NiO.

However, as shown in Figure 3, the N 2p states exhibit a very weak interaction with the O 2p and Ni 3d states with respect to C 2p states, which can be responsible for why N doping leads to less band gap narrowing than C doping. To elucidate the underlying reason for this observation, we plotted the electron density difference maps (between doped and pure NiO) along a (100) plane in N- and C-doped NiO in Figure 4. We find that the charge character of the N 2p states shows a very weak interaction with the neighboring O and Ni atoms (cf. Figure 4(a)). Figure 4(b) shows that the charge density difference of the C 2p states exists in conjunction with some coupling with the Ni 3d states. Such an interaction between the dopant C and its neighbouring host Ni atoms is more apparent than that of N-doped NiO, which leads to isolated C 2p gap states responsible for the reduction of electron transition energy.

In conclusion, based on first-principles calculations and analysis of the electronic

structures of N- and C-doped NiO, it was found that both impurities N and C induce their 2p impurities states in the band gap and locate at the conduction band minimum, which can narrow the band gap significantly. However, based on these results, it would be expected that N-doped NiO would exhibit a higher degree of photocatalytic efficiency than that of C-doped NiO under visible-light irradiation because of the presence of recombination centres for carriers in C-doped NiO. These results indicate that N-doped NiO could serve as a promising photocatalytic material.

Acknowledgements

The authors thank Dr. Michael Nolan for useful discussions. This work was supported by the Irish Research Council for Science, Engineering and Technology (IRCSET). The authors thank both Science Foundation Ireland and the HEA/SFI-supported Irish Centre for High End Computing (ICHEC) for the provision of High Performance Computing facilities.

References

[1] V. E. Henrich, P. A. Cox, *The Surface Science of Metal Oxides*; Cambridge University Press: Cambridge, England, 1994.

[2] A. L. Linsebigler, G. Lu, J. T. Yates, Chem. Rev. 95 (1995) 735

[3] R. Asahi, T. morikawa, T. Ohawaki, K. Aoki, Y. Taga, Science 293 (2001) 269.

[4] H. Irie, Y. Watanabe, K. Hashimoto, J. Phys. Chem. B 107 (2003) 5483.

[5] X. B. Chen, C. Burda, J. Am. Chem. Soc. 130 (2008) 5018.

[6] V. E. Henrich, P. A. Cox, *The Surface Science of Metal Oxides*; Cambridge University Press: Cambridge, England, 1994.

[7] A. L. Linsebigler, G. Lu, J. T. Yates, Chem. Rev. 95 (1995) 735

[8] Z. G. Zou, J. H. Ye, K. Sayama, H. Arakawa, Nature 625 (2001) .

[9] C. Hu, X. X. Hu. J. Guo, and J. H. Qu, Environ. Sci. Technol, 40 (2006) 5508.

[10] J. J. Zou, C. J. Liu, and Y. P. Zhang, Langmuir 22 (2006) 2334.

[11] E. Jerndal, T. Mattisson, and A. Lyngfelt, Energy & Fuels 23 (2009) 665.

[12] H. Bo Zhao, L. M. Liu, B. W. Wang, D. Xu, L. L. Jiang, and C. G. Zheng, Energy & Fuels 22 (2008) 898.

[13] Cox, P. A. *Transition Metal Oxides: An Introduction to their Electronic Structure and Properties*; The International Series of Monographs on Chemistry Vol. 27; Claredon Press: Oxford, U.K., 1995.

[14] G. Kresse, J. Hafner, Phys. Rev. B 47 (1994) 558.

[15] G. Kresse, J. Furtherműller, Phys. Rev. B 54 (1996) 11169.

[16] J. P. Perdew, K. Burk, M. Ernzerhof, Phys. Rev. Lett. 77 (1996) 3865.

[17] J. P. Perdew, Y. Wang, Phys. Rev. B 45 (1992) 13244.

[18] H. J. Monkhorst, J. D. Pack, Phys. Rev. B 13 (1976) 5188.

[19] S. L. Dudarev, G. A. Botton, S. Y. Savarsov, C. J. Humphreys, A. P. Sutton, Phys. Rev. B, 57 (1998) 1505

[20] N. Yu, W. B. Zhang, N. Wang, Y. F. Wang, and B. Y. Tang, J. Phys. Chem. C 112 (2008) 452.

[21] I. de P. R. Moreira, F. Illas, and R.L. Martin, Physical Review B 65 (2002) 155102.

[22] G. A. Sawatzky, J. W. Allen, Phys. Rev. Lett. 53 (1984) 2339.

[23] A. K. Cheetham, D. A. O. Hope, Phys. Rev. B 27 (1983) 6964.

[24] S. Hufner, J. Osterwalder, T. Riesterer, F. Hulliger, Solid State Commun. 52 (1984) 793.

[25] R. Long, N. J. English, Appl. Phys. Lett. 94 (2009) 132102.

[26] *CRC Handbook of Chemistry and Physics* 87th ed.; Lide, D. R.Taylor & Francis: London, 2006.

[27] G. Henkelman, A. Arnaldsson, and H. Jónsson, Comput. Mater. Sci. 36 (2006) 254.

Table 1. Band gap, lattice constant, magnetic moment of Ni **solid** from GGA + U compared with experiments.

	Band gap (eV)	**Lattice constant(Å)**	**Magnetic Moment(μB)**
GGA + U	*2.6*	*4.16*	*1.68*
experiment	*3.8*[a]	*4.17*[b]	*1.64*[c]

[a]Ref. 13. [b]Ref. 22. [c]Ref.23.

Table 2 Formation energies (eV) of N- and C-doped NiO.

E_{form}	**O-rich**	**Ni-rich**
N@O	*6.5*	*3.0*
C@O	*12.5*	*9.0*

Figure Captions

Figure 1. Supercell model for defective anatase showing the location of the dopants. The ion doping sites are marked with X (N, C). The large dark spheres and the small light spheres represent the Ni and O atoms, respectively.

Figure 2. (a) DOS and (b) PDOS for pure NiO. The valence band maximum is set to zero.

Figure 3. DOS (left panel) for N@O and C@O (red) compared with pure NiO (black) and PDOS for impurity atoms (red). The valence band maximum of pure NiO is taken as the reference level. The dashed lines represent the Fermi level E_F.

Figure 4. Electron density difference along the (100) plane in doped NiO of (a) N@O , and (b) C@O.

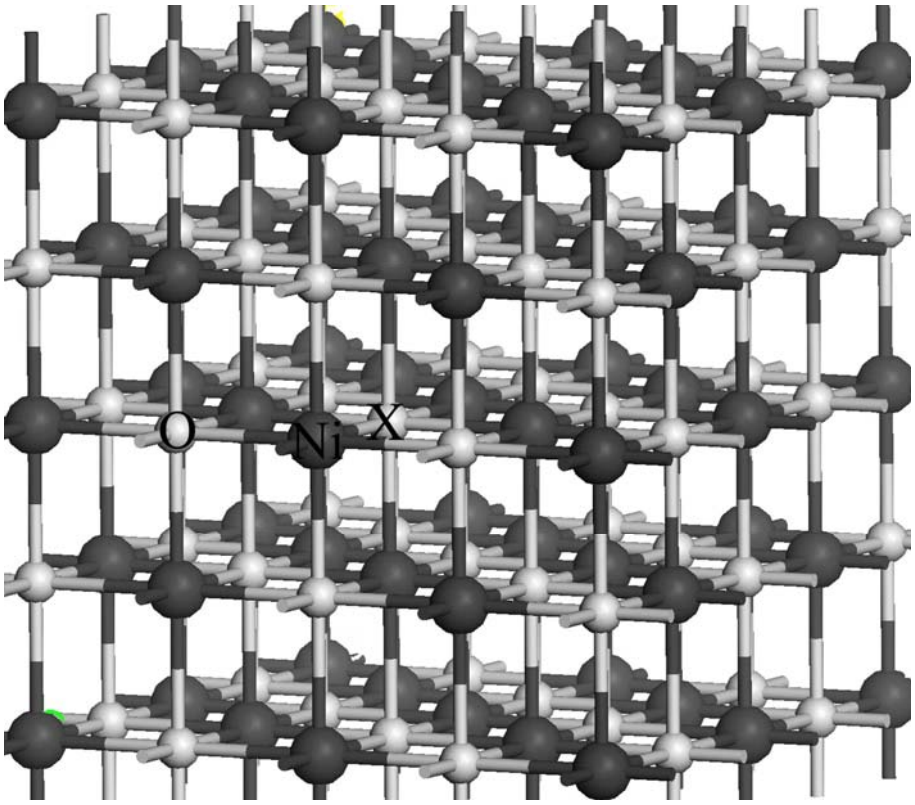

Figure 1

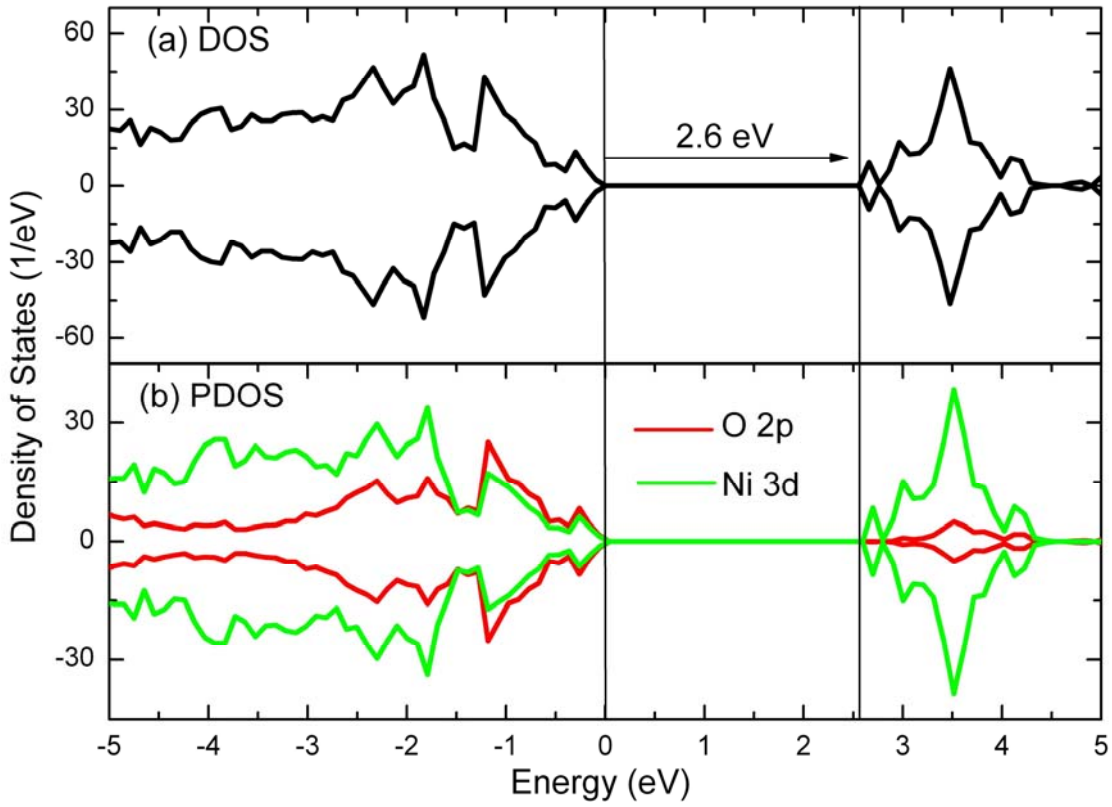
(a) DOS
2.6 eV
(b) PDOS
O 2p
Ni 3d
Density of States (1/eV)
Energy (eV)
60
30
0
-30
-60
-5
-4
-3
-2
-1
0
1
2
3
4
5

Figure 2

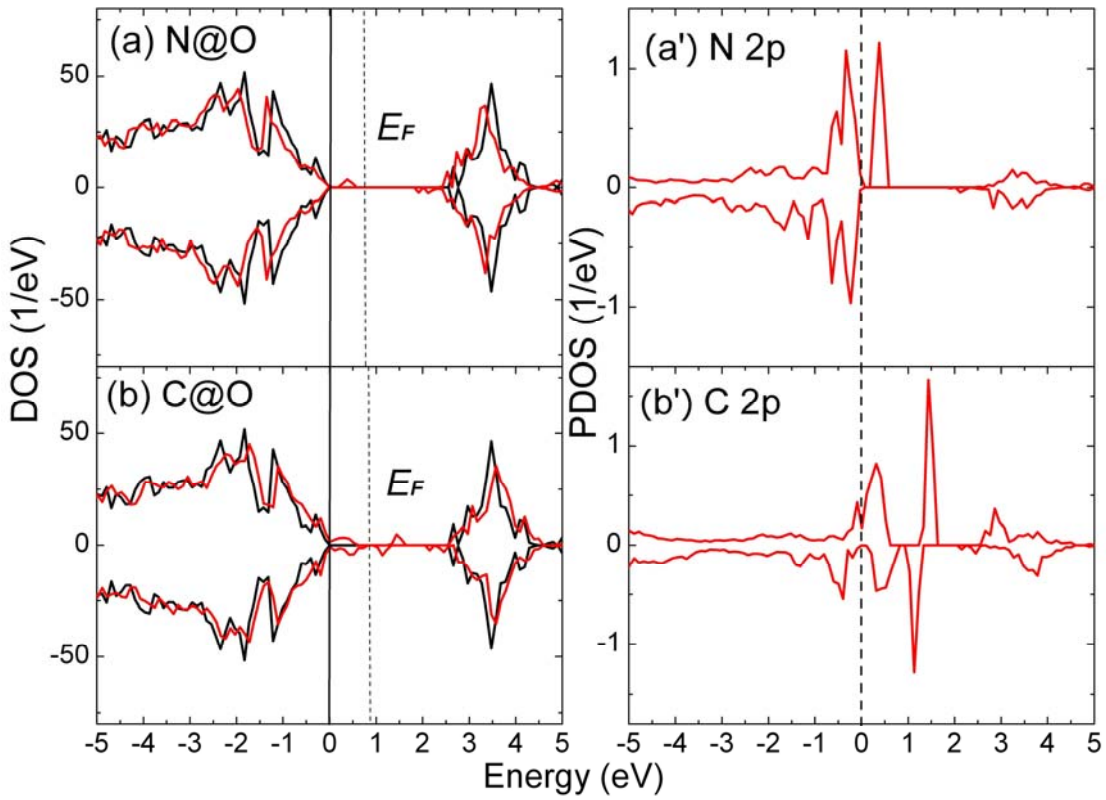
(a) N@O
(b) C@O
(a') N 2p
(b') C 2p
E_F
E_F
DOS (1/eV)
PDOS (1/eV)
Energy (eV)
50
0
-50
1
0
-1
-5 -4 -3 -2 -1 0 1 2 3 4 5

Figure 3

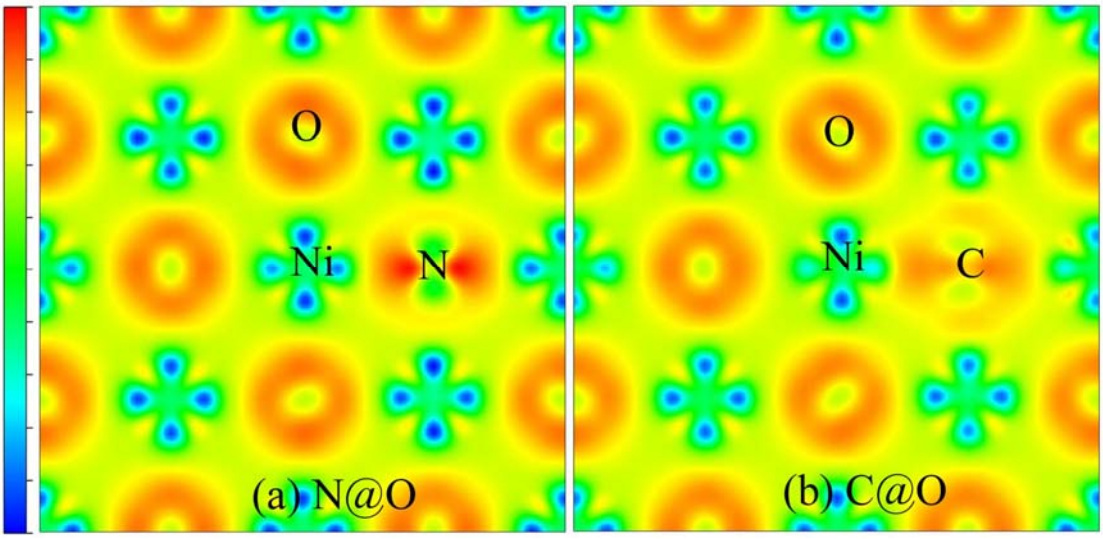

Figure 4